EUROFUSION WPS1-PR(16) 15310

G. A. Wurden et al.

A High Resolution IR/Visible Imaging System for the W7-X Limiter

Preprint of Paper to be submitted for publication in
21st Topical Conference on High Temperature Plasma
Diagnostics 2016

This work has been carried out within the framework of the EUROfusion Consortium and has received funding from the Euratom research and training programme 2014-2018 under grant agreement No 633053. The views and opinions expressed herein do not necessarily reflect those of the European Commission.

A High Resolution IR/Visible Imaging System for the W7-X Limiter [a)]

G. A. Wurden,[1,b] L. A. Stephey,[2] C. Biedermann[3], M. W. Jakubowski[3], J. P. Dunn[1], M. Gamradt[3], and the W7-X Team[3]

[1]*Los Alamos National Laboratory, Los Alamos, NM 87545, USA*
[2]*Universition of Wisconsin, Madison, WI 53706, USA*
[3]*Max Planck Institut für Plasma Physik, Wendelsteinstrasse 1, 17491 Greifswald, Germany*

(Presented June 5, 2016; received xxx; accepted xxx; published online xxx)

A high-resolution imaging system, consisting of megapixel mid-IR and visible cameras along the same line of sight, has been prepared for the new W7-X stellarator, and was operated during Operational Period 1.1 (OP1.1) to view one of the five inboard graphite limiters. The radial line of sight, through a large diameter (184 mm clear aperture) uncoated sapphire window, couples a direct viewing 1344x784 pixel FLIR SC8303HD camera. A germanium beam-splitter sends visible light to a 1024x1024 pixel Allied Vision Technologies Prosilica GX1050 color camera. Both achieve submillimeter resolution on the 161 mm wide, inertially-cooled, segmented graphite tiles. The IR and visible cameras are controlled via optical fibers over full Camera Link and dual GigE Ethernet (2 Gbit/second data rates) interfaces, respectively. While they are mounted outside the cryostat at a distance of 3.2 meters from the limiter, they are close to a large magnetic trim coil, and require soft iron shielding. We have taken IR data at 125 Hz to 1.25 kHz frame rates, and seen surface temperature increases in excess of 350 °C, especially on leading edges or defect hot spots. The IR camera sees heat-load stripe patterns on the limiter, and has been used to infer limiter power fluxes (~1 to 4.5 MW/m^2), during the ECRH heating phase. IR images have also been used calorimetrically between shots to measure equilibrated bulk tile temperature, and hence tile energy inputs (in the range of 10 kJ/tile with 4 MW, 300 millisecond heating pulses). Small UFO’s can be seen and tracked by the FLIR camera in some discharges. The calibrated visible color camera (100 Hz frame rate) has also been equipped with narrow band C-III and H-alpha filters, to compare with other diagnostics, and is used for absolute particle flux determination from the limiter surface. Sometimes, but not always, hot-spots in the IR are also seen to be bright in C-III light.

I. INTRODUCTION

Preparations for the first Wendelstein 7-X plasmas in 2016 have been under development for many years[1]. Diagnostic sets have been well-defined, and many of the 150 ports on W7-X are already used or occupied[2]. As part of the US-German 3-Lab collaboration (LANL/ORNL/PPPL) on W7-X, we have an interest in edge plasma interactions with the wall in 3D geometry. LANL in particular was looking at supplementing the extensively planned wide-angle visible/IR endoscopes for machine safety for the later operating phases of W7-X. A state-of-the art FLIR high resolution mid-IR camera and data acquisition system (which we first tested at Alcator C-Mod[3]) was shipped to Germany in 2013 from the USA, for prototype testing and software development. As late as 2014, it was not feasible to install any new diagnostic with in-vessel optics, and still meet the vessel closure schedule. However, in the summer of 2014, we realized that one pair of ports (designated in future years for an ICRH antenna), would have a direct view of the Module 3 poloidal graphite limiter, given a big enough window. The lower port (AEA30) was easily accessible from the decking surrounding W7-X (8 meters above torus hall floor), and furthermore there luckily was space reserved for future maintenance of one of the five American trim-coils, which we could instead use for mounting a new diagnostic. We were even able to go inside, the vessel to confirm that the unused ports hadn’t been covered over by protective stainless plating (but were simply plugged with a rubber cover during construction). This was the origin of the high-resolution combined IR/visible diagnostic presented in this paper, which was successfully installed and operated for the first W7-X plasmas in 2015-2016.

II. EXPERIMENTAL ARRANGEMENT

The infrared and visible cameras share an identical line of sight towards the limiter, looking through a 215 mm diameter (6 mm thick) uncoated sapphire metal-sealed (Helicoflex) vacuum window. No shutter was employed (we relied on a distance of 1.5 meters from the plasma to

---

[a)] Contributed paper published as part of the Proceedings of the 21th Topical Conference on High-Temperature Plasma Diagnostics, Madison, Wisconsin, June 2016.

[b)] Author to whom correspondence should be addressed:

window to avoid plasma contamination) and the window assembly could easily withstand more than the 150 ºC bake-out temperatures employed at W7-X.

We mounted a FLIR SC8303HD 3-5 um infrared camera operating at 125 Hz (for a full frame of 1344x784 pixels, or even faster if sub-windowed), communicating over a fiber-optic full EDT Camera Link interface to the Dell T5600 acquisition workstation (with Teledyne DALSA Xcelera-CL PX4 frame-grabber, 64 Gb RAM, 2 Tb hard disk, NVIDIA Tesla GPU board), located about 100 meters away in basement diagnostic racks. The FLIR camera was either equipped with an f/4 50 mm or 200 mm germanium lens. For IR calibration, we had pre-calibrated lenses from FLIR, but we also used an HGH Infrared Systems ECN100 large area flat field source to 500 ºC, and an HGH RCN high temperature black body cavity source, up to 1200 ºC.

FIG. 1. CAD and actual view of IR & visible camera installation on the AEA30 port of W7-X. The iron shield box (just beyond the railing) encloses both the IR and visible camera, and is adjacent to one of the five external magnetic trim coils.

The Allied Vision Technologies Prosilica GX1050C color visible camera used a twin GigE fiber-optic Ethernet interface, to transfer 1024x1024 pixel RGB images @ 100 Hz to a second acquisition computer. An Interference filter was placed in front of the 50 mm f/1.4 C-mount visible lens, and could be swapped out daily, as desired. An NBS-traceable visible light source and integrating sphere was used for absolute visible camera calibrations. A spatial resolution of 1 mm at the limiter was achieved with both systems.

Because of the close proximity to the magnetic trim coil (brown object in Figure 1), we were concerned about magnetic field effects on the cameras. In fact, we tested them (to the point of failure) in the magnetic field of the VINETA linear machine[4] at the IPP. We found a transverse field of 25 mTesla caused Ethernet interfaces to fail, while the Stirling engine on the IR camera would fail by 60 mTesla. For an axial B-field (along the line of the camera lens to camera body), both the FLIR camera cooling engine and its Camera Link interface worked up to 80 mTesla, if not shielded. Consequently, as a compromise, we employed a soft iron shield, 6 mm thick, (but open for the two lenses on the front), and completely open (for forced air cooling) on the back. It reduced the local B-field to < 1.2 mTesla. The effect of 10 kG of iron on the plasma edge was calculated[5] to be < $4x10^{-7}$. No magnetic field perturbations on the cameras were noticed during the experiments.

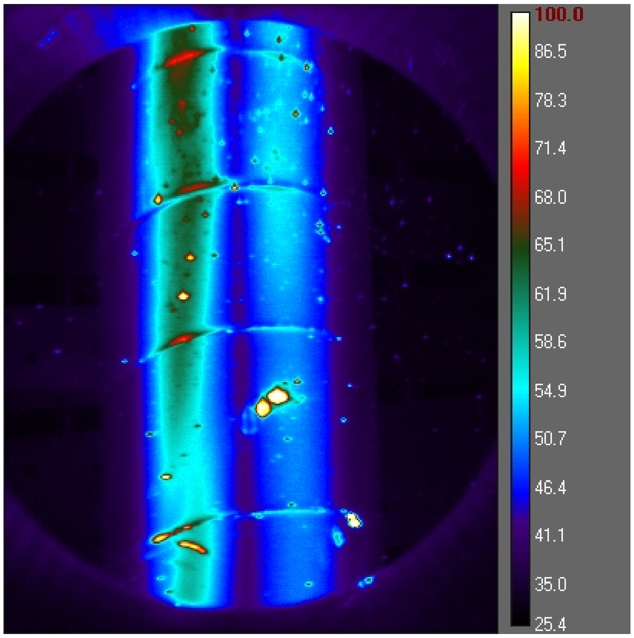

FIG. 2. Shot 160121004 IR temperature (ºC) image, during a 4.3 MW 6-gyrotron helium discharge, 125 msec into the 250 msec plasma pulse, at 453 Hz framing rate, 0.5 msec exposure. This shows the typical dual heat stripe temperature pattern on the graphite limiter during a standard iota discharge. Note the increased temperature of the leading edge of each tile on the left stripe, and also hotspots.

The combined data rate for these mega-pixel cameras is 4 Gigabits/second. We used FLIR ResearchIR software[6] for the infrared acquisition, and MATLAB routines for the visible camera. IR data was archived locally, while the visible data was uploaded across the network to MDSPlus. Later we plan to do real time hot spot detection with compiled MATLAB routines by pulling images from the IR data stream to the NVIDIA GPU onboard memory (6GB RAM), and divide up the processing to 2048 (or more) processors, to achieve 1 second or better response time.

III. INFRARED IMAGING

We obtained ¼ Terabyte of IR images during OP1.1 operations, consisting in total of more than 400 regular discharges, and 1300 conditioning (short high power cleaning) pulses. In Figure 2, we show a typical dual heat stripe pattern on the graphite limiter, with FWHM of each stripe ~ 4.5 cm. To first order, including the left-right and up-down asymmetries, this pattern was predicted[1] by EMC3-Eirene modeling for the standard iota configuration of the plasma edge that W7-X used for most of OP1.1. Further details, not in the modelling, include observation of increased heating of leading edges of the tiles, on the bottom edge of each tile on the left stripe, and on the top edge of each tile, on the right stripe. This is however consistent with the local field line direction.

IV. VISIBLE IMAGING

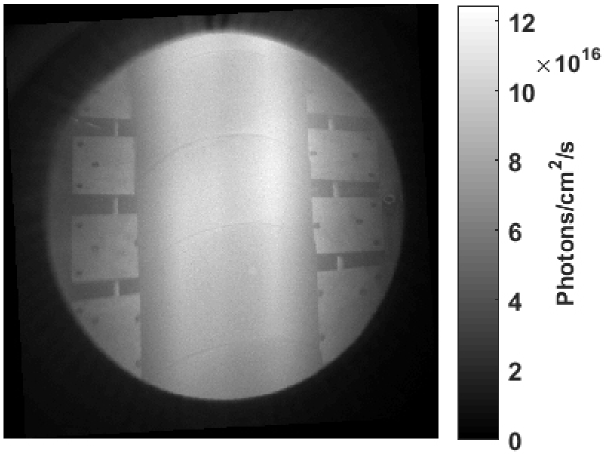

FIG. 3. Shot 160121004. This filtered CIII (465 nm) image (5 msec exposure) shows dual stripes during a helium ECRH plasma in Wendelstein 7-X. Copper backing plates (and threaded holes) can be seen to the left and right sides of the limiter.

Broadband and narrowband-filtered images of the limiter were obtained with the RGB visible camera described above and in detail in reference [7]. Generally during helium plasmas, a C-III (465 nm) filter was used with a 3 nm FWHM and 70% transmission. During hydrogen plasmas, an H-alpha (656 nm) filter was used with a 5 nm FWHM and 70% transmission. In both cases two vertical stripes of enhanced photon emission were observed in approximately the same locations as those seen in the infrared, as shown in Figure 3. Differences in emission pattern between the visible and infrared data can be attributed both to the dependence of photon emission on local plasma parameters and the effective photon integration over the chosen line of sight.

A Labshpere model UK2 integrating sphere was used to absolutely calibrate the entire optical system. The calibration was performed on the bench after the experimental campaign. All experimental parameters were unchanged with the exception of the substitution of a smaller but equivalent sapphire window. A calibration matrix for filter type, camera gain and exposure time (generally between 1-9 ms) was developed to allow the measured counts to be converted into a photon flux. The system was calibrated with the same data acquisition setup as was used in the experiment.

Ultimately this measured visible photon flux will be used to determine a limiter particle flux in conjunction with a synthetic diagnostic developed for EMC3-EIRENE[8]. This is necessary to interpret the somewhat more complex spectroscopic data.

V. ACKNOWLEDGEMENTS

We wish to thank especially Hans-Stefan Bosch, Ralf König, Thomas Sunn Pedersen, Thomas Klinger, and the entire W7-X Team for supporting and enabling the preparation of this diagnostic in time for the first plasmas on W7-X. This work has been funded under DOE LANS Contract DE-AC52–06NA25396, and Office of Science DE-SC0014210. This work has also been carried out within the framework of the EUROfusion Consortium and has received funding from the Euratom research and training program 2014-2018 under grant agreement No 633053.

VI. REFERENCES

1. T. S. Pedersen, T. Andreeva, H. S. Bosch, S. Bozhenkov, F. Effenberg, et. al., and W.-X. Team, Nucl Fusion **55** (12) (2015).
2. R. Konig, J. Baldzuhn, W. Biel, C. Biedermann, et. al. and W.-X. Team, J Instrum **10** (2015).
3. G. A. Wurden and J. L. Terry, B Am Phys Soc **57** (12), JP8.92 (2012).
4. H. Bohlin, A. Von Stechow, K. Rahbarnia, O. Grulke and T. Klinger, Rev Sci Instrum **85** (2) (2014).
5. T. Andreeva, R. Brakel, J. Kisslinger and M. Koeppen, 42nd European Physical Society Conference on Plasma Physics, **Poster P1.162** http://ocs.ciemat.es/EPS2015PAP/pdf/P1.162.pdf , Lisbon, Portugal (2015).
6. FLIR, ResearchIR software, http://www.flir.com/science/display/?id=51371 (2015).
7. L. Stephey, G. A. Wurden, O. Schmitz, et al., this conference, Rev Sci Instrum HTPD, 2016.
8. Frerichs, H., F. Effenberg, O. Schmitz, et al. , this conference, Rev Sci Instrum HTPD, 2016.